electronic reprint

Journal of
Applied Crystallography
ISSN 0021-8898
Editor: **Gernot Kostorz**

PRINSAS – a Windows-based computer program for the processing and interpretation of small-angle scattering data tailored to the analysis of sedimentary rocks

Alan L. Hinde

Journal of
Applied
Crystallography
ISSN 0021-8898

Received 14 November 2003
Accepted 31 August 2004

PRINSAS – a Windows-based computer program for the processing and interpretation of small-angle scattering data tailored to the analysis of sedimentary rocks

Alan L. Hinde

Geoscience Australia, GPO Box 378, Canberra, ACT 2601, Australia. Correspondence e-mail: alan.hinde@ga.gov.au

PRINSAS is a Windows program that takes as input raw (post-reduction) small-angle neutron and small-angle X-ray scattering (SANS and SAXS) data obtained from various worldwide facilities, displays the raw curves in interactive log–log plots, and allows processing of the raw curves. Separate raw SANS and ultra-small-angle neutron scattering (USANS) curves can be combined into complete scattering curves for an individual sample. The combined curves can be interpreted and information inferred about sample structure, using built-in functions. These have been tailored for geological samples and other porous media, and include the ability to obtain an arbitrary distribution of scatterer sizes, the corresponding specific surface area of scatterers, and porosity (when the scatterers are pores), assuming spherical scatterers. A fractal model may also be assumed and the fractal dimension obtained. A utility for calculating scattering length density from the component oxides is included in the program.

1. Overview

The program *PRINSAS* (Hinde, 2002) is a Windows program that allows data obtained from the small-angle scattering of neutrons and X-rays to be displayed, processed and interpreted. It is designed to handle data from pinhole geometry, time of flight (TOF) and Bonse–Hart machines and has been tested using data acquired from several specific instruments, as listed in Table 1. It is assumed that initial corrections for sample thickness, transmission, quantum efficiency of the detector, and noise have been made according to general rules, at the facility, and that at least some of the data (*i.e.* for at least one sample-to-detector distance) are in absolute units.

The program was written with the interpretation of scattering results for sedimentary rocks in mind, but may be used for any small-angle scattering data. In designing the program, ease of use, user interaction and visual display of data were the major considerations. Error values can be displayed but are not taken into account in the analysis routines. The program is written in Microsoft Visual Basic and makes use of embedded Microsoft *Excel* charts for the interactive display of the scattering data, and the *Excel* addin 'Solver' for some routines. The data are input from raw data files, or manually entered, and stored in Microsoft *Access* databases. Use of the program does not require knowledge of Microsoft *Access*, although familiarity with *Excel* is an advantage. Data are easily exported to *Excel* workbooks for further analysis.

Use of the program is divided into two stages: (i) the entry and initial processing of raw (post-reduction) small-angle neutron scattering (SANS) [including ultra-small-angle scattering (USANS)] and small-angle X-ray scattering (SAXS) data to produce curves of intensity *versus* scattering vector, defined in equation (1) [$I(Q)$ *versus* Q], and (ii) the interpretation and analysis of the $I(Q)$ curves to infer structural information about the samples being studied. This includes information about the nature of the sample, such as the scatterer size distribution and specific surface area of scatterers, assuming spherical scatterers, as well as the fractal dimension if a (surface) fractal model is assumed. Fig. 1 shows the tasks within these two stages that the program is designed to perform.

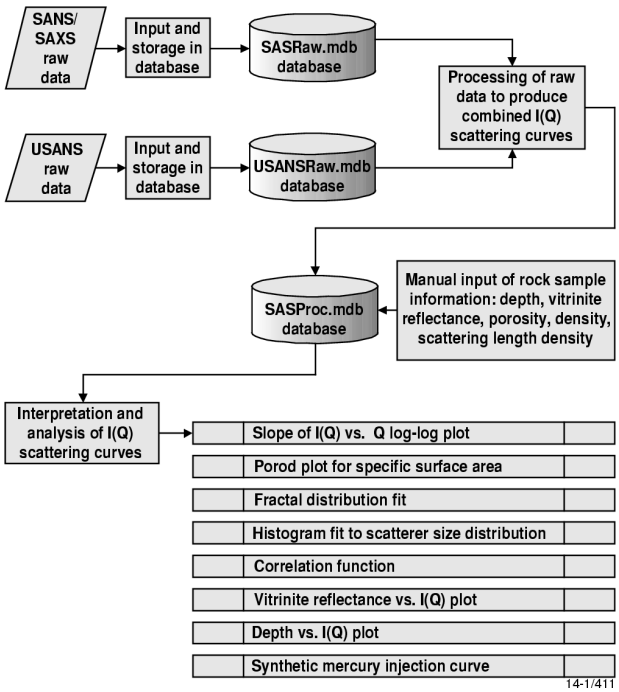

Figure 1
Overview of the program *PRINSAS* showing the stages of raw data processing and subsequent interpretation.

Table 1
Major facilities that provide small-angle scattering data.

Facility	Instrument name	Wavelength	Type of data produced
IPNS (Intense Pulsed Neutron Source at Argonne National Laboratory, Illinois, USA)	SAND	0.5 Å to 14 Å, time-of-flight	SANS, SANSS,† SANSW
ILL (Institute Laue-Langevin in Grenoble, France)	D11 (pinhole)	4.5 Å to >15 Å	SANS
Grenoble Research Reactor, Grenoble, France	S18, Neutron Interferometer and USANS	1.96 Å	USANS
ORNL (Oak Ridge National Laboratory, Ts, USA)	18m SANS (pinhole)‡	4.75 Å	SANS
	USANS‡	2.59 Å	USANS
	14m SANS§	4.75 Å	SANS
	10m SAXS	Cu $K\alpha$	SAXS
NIST (National Institute of Science and Technology, Md, USA)	NG3, NG7 (pinhole)	5 Å to 20 Å	SANS

† SANSS − SANS small angle, SANSW − SANS data acquired using the wide-angle detector bank. ‡ Now decommissioned. § Being upgraded in 2001–2002.

Stage (i) is used to input data (and was tested on data) obtained from five different small-angle scattering instruments (see Table 1). For pinhole-geometry machines, raw data are generally provided as three sets of data in three adjacent Q ranges; the program joins the three sets and allows them to be aligned. USANS data from ORNL and the Grenoble S18 instrument require additional processing and correction, which is handled by the program. The subtraction of background and desmearing of USANS data is also handled at this stage.

In stage (ii), the processed data can be fitted with models that enable the specific surface area, spherical scatterer size distribution and porosity (if the scatterers are pores) to be calculated.

No allowance for multiple scattering is made in *PRINSAS* and the user is alerted to the fact that multiple scattering may affect the scattering data, especially for USANS and for thick samples. Methods for taking into account the effects of multiple scattering are available in the literature (*e.g.* Sabine & Bertram, 1999; Schelten & Schmatz, 1980).

The purpose of this paper is to describe *PRINSAS* (version 2.0) and its capabilities. It represents the research needs of our group. Further development of the program is possible depending on future research needs and feedback. Detailed instructions for running the program are contained in the online help provided with the program. The program can be downloaded, free of charge, from http://www.ga.gov.au/about/corporate/ga_authors/publications_free.jsp#Marine (or search http://www.ga.gov.au/ for 'PRINSAS').

2. Background theory

2.1. Absolute scattering intensity

The theory of small-angle scattering is well described in the literature, both generally (Guinier *et al.*, 1955; Espinat, 1990; Lindner & Zemb, 1991) and specifically for geological applications (Bale & Schmidt, 1984; Wong *et al.*, 1986; Mildner & Hall, 1986; Radlinski *et al.*, 1996; Radlinski & Radlinska, 1999; Radlinski & Hinde, 2001). Only the equations relevant to the program are reproduced here.

The absolute scattering intensity per unit volume for a sample containing a volume fraction φ of monodisperse spheres of radius r is given by

$$\frac{\mathrm{d}\Sigma}{\mathrm{d}\Omega} \equiv I(Q) = (\rho_1 - \rho_2)^2 \varphi(1-\varphi) V_r F_{\mathrm{sph}}(Qr), \quad (1)$$

where $Q = 4\pi\sin\theta/\lambda$ is the scattering vector magnitude (θ is the scattering angle and λ is the wavelength); the scattering contrast is

$$\overline{\Delta\rho^2} = (\rho_1 - \rho_2)^2 \varphi(1-\varphi), \quad (2)$$

where ρ_1 and ρ_2 are the scattering length densities of the two phases; the volume of an individual pore is $V_r = (4/3)\pi r^3$; and the form factor for a sphere of radius r is

$$F_{\mathrm{sph}}(Qr) = \left[3\frac{\sin(Qr) - Qr\cos(Qr)}{(Qr)^3}\right]^2. \quad (3)$$

2.2. Experimentally measured scattering intensity

In an experimental situation, the measured intensity is affected by several instrumental and sample-specific parameters and is related to the absolute intensity, equation (1), by the equation

$$I(Q)_{\mathrm{meas}} = I_0 A t T \frac{\mathrm{d}\Sigma}{\mathrm{d}\Omega}\mathrm{d}\Omega E(\theta,\lambda) + \mathrm{bkg}, \quad (4)$$

where I_0 is the incident beam intensity, A is the surface area of the sample, t is the thickness of the sample, T is the sample transmission, $\mathrm{d}\Sigma/\mathrm{d}\Omega$ is the scattering intensity $I(Q)$, $\mathrm{d}\Omega$ is the solid angle at scattering vector Q, $E(\theta,\lambda)$ is the quantum efficiency of the detector array, and bkg is the background.

$I(Q)_{\mathrm{meas}}$ is routinely reduced to $I(Q)$, using equation (4), at the small-angle scattering facilities. *PRINSAS* therefore only uses these $I(Q)$ data sets. For a further discussion of experimentally measured scattering curves see, for example, Strunz *et al.* (2000).

3. Overview and capabilities of the program *PRINSAS*

Fig. 1 shows an overall flow chart of the program: the tasks it is designed to do and its relation to the *Access* databases in which it stores the data.

3.1. Input and storage of raw data

Raw data, obtained from various laboratories, are generally in the form of text files, which vary in format. The facilities produce for each sample a maximum of three sets of data, each with a different Q range. The program can accept raw SANS data files from ORNL, Argonne and NIST, raw USANS data files from ORNL, and pre-processed USANS data files from instrument S18 at the Grenoble Research Reactor. The program can also read data from a text file prepared in a format specific to the program. This file must be created by the user and can be used for entering data in formats not recognized by the program. Data can also be entered directly into the program.

The raw data are stored in one of two *Access* databases. The first database, SASRaw.mdb, is for SANS and SAXS data. The second, USANSRaw.mdb, is for USANS data. Each database has its own type of window for displaying the data. The units used by the program when displaying the data are $\mathrm{Å}^{-1}$ for Q and cm^{-1} for $I(Q)$.

For SANS and SAXS data, the program accepts up to three sets of data for each sample. For USANS data, up to three sets of raw data, or one set of 'pre-processed' data may be provided. Pre-processing is described in a user manual provided by ORNL (*USANS User Manual*, 1999). Additional data that can be entered into the program to aid analysis include the sample thickness and wavelength of the beam, and descriptive data for the sample.

Table 1 lists the characteristics of five instruments from which small-angle scattering data can be obtained.

3.2. Processing the raw data

The raw data for a single sample can be displayed in a window specific to its database (SASRaw or USANSRaw). This window displays, in a drop-down list, all the samples in its database. After selecting a sample, a log–log plot of the raw data appears. For SASRaw data, and USANSRaw data that have not been processed, up to three sets of data appear. In cases where the adjacent data sets overlap, cutoff values of Q are used to separate the two sets. These cutoff values are displayed as vertical lines and may be moved with the mouse. The optimum location must be judged by eye to give a smooth combined curve with minimal noise.

The first stage of processing is to align the data sets. This is done by clicking and vertically dragging a data set with the mouse, or by using in-built routines designed to align adjacent datasets automatically.

The next stage is to subtract a background value from each data point. A horizontal line that represents the background value appears on the plot and may be dragged with the mouse until the resulting scattering curve is corrected, for example, when the large-Q end of the scattering curve becomes linear (on a log–log scale) as is expected in the Porod limit. There is a built-in routine to determine the background automatically by making the large-Q end of the scattering curve as linear as possible. For USANS data, there is a choice of making the large-Q end linear (on a log–log scale), or of matching the slope of a fitted line to a specific value, typically a value that will match (after desmearing) the corresponding SANS data to which it will later be joined. Note that the slope at the large-Q end becomes less negative by a value of one after desmearing. The ability to display straight lines fitted to the $I(Q)$ curves, as well as the corresponding slopes, is also provided.

USANS data may require the additional stage of subtracting the scattering curve for an empty cell, and of desmearing. Approximate propagated error values are calculated for subtracting the empty-cell values and desmearing. Desmearing corrects for the geometry of the slit through which the neutrons are passed before being scattered by the sample. The assumed geometry is an infinitely thin slit.

The desmearing process is an automatic iterative process based on the method of Lake (1967). The user, however, must decide at which point to stop as the desmeared curve gradually becomes more noisy after a few iterations. Some options are available for fine tuning the numerical process in difficult cases that will not converge.

The final stage is to store the processed data in the SASProc database. This is used to store the collection of processed SANS (and SAXS) and USANS scattering curves as well as the curves obtained by combining SANS and USANS data for specific rock samples. The combined curves can be interpreted and analysed by methods described below.

3.3. Interpretation of the processed data

Processed $I(Q)$ scattering curves stored in the SASProc database are displayed in a window that allows the simultaneous display of up to five scattering curves at one time.

3.3.1. Joining SANS and USANS data. The scattering curves for samples having both SANS and USANS data can be joined and saved in the SASProc database as single $I(Q)$ curves. The SANS and USANS data must first be displayed simultaneously, aligned, and Q-cutoff values set if there is any overlap. The curves may be aligned by dragging the USANS curve with the mouse or by running a built-in alignment routine similar to those described for raw data. Individual data-point outliers may be removed before the combined data are saved.

3.3.2. Manual input of rock-sample information. In addition to data that are stored in the SASProc database automatically, a number of properties, tailored for studying sedimentary rocks, may be entered manually. These include a description of the sample, its depth, vitrinite reflectance, porosity, density and scattering length density. Depth and vitrinite reflectance are required for the depth *versus* $I(Q)$ and vitrinite reflectance *versus* $I(Q)$ plots described below.

3.3.3. Slope of *I*(*Q*) *versus* *Q* plot. The smoothness of a scattering curve may be visually assessed using a plot of slope of $I(Q)$ *versus* Q on a log–log scale. This plot is displayed in a separate window. The slope is determined for adjacent sections of the curve, each section consisting of a constant number of data points. This number is called the 'stepping average' and can be changed on the plot. The smoothness or jaggedness of this plot may lead to a reconsideration of how sets of SANS and USANS data are joined; that is, how much USANS data are offset relative to SANS data as described above.

3.3.4. Porod plot for specific surface area. A plot of $Q^{6-f_D}I(Q)$, where f_D is the fractal dimension of the sample, *versus* Q can be used to determine the specific surface area of the sample, assuming a surface fractal. The Q range should be limited to the straight region of the $I(Q)$ curve from which f_D is calculated using its slope ($f_D = 6 +$ slope). The length scale and density contrast are specified in the Porod plot window. The theory behind fractal structures is described further below.

3.3.5. Fractal distribution fit. Scattering curves for samples that have a fractal structure of scatterers are linear (on a log–log scale) in the large-Q region. For surface fractals, the slope of the linear region is $-(6 - f_D)$ (Schmidt, 1989). A sample composed of a polydisperse distribution of scattering spheres (a porous rock for example), where the probability density function of the sphere radii is proportional to $r^{-(1+f_D)}$, also has a linear $I(Q)$ region with this slope. Expressed mathematically,

$$I(Q) = (\rho_1 - \rho_2)^2 \frac{\varphi}{\overline{V}_r} \int_{R_{\min}}^{R_{\max}} V_r^2 f(r) F_{\rm sph}(Qr)\,{\rm d}r, \qquad (5)$$

where $\overline{V}_r = \int_0^\infty V_r^2 f(r)\,{\rm d}r$ is the average pore volume and

$$f(r) = \frac{r^{-(1+f_D)}}{(R_{\min}^{-f_D} - R_{\max}^{-f_D})/f_D}. \qquad (6)$$

Although analytical solutions exist for equation (5) (*e.g.* Mildner & Hall, 1986), they are derived from and based on assumptions about the correlation function that may not correspond to nature and do not explicitly take into account the range $R_{\min}$ to $R_{\max}$. *PRINSAS* finds the fractal distribution using numerical integration to evaluate equation (5), and *Excel*'s built-in Solver routine to find the optimum parameter values by non-linear least squares. The fitting procedure can determine values for $R_{\min}$, $R_{\max}$, f_D and $I(0)$. A separate *Excel* worksheet is created and the fit is achieved by running Solver.

3.3.6. Histogram fit of pore size distribution. The fractal distribution fit assumes a specific functional form for the pore size distribution. A more general distribution can be determined by expressing the distribution as a histogram,

$$I(Q) = \sum_i IQ_{0i} \frac{\int_{R_{\min_i}}^{R_{\max_i}} V_r^2 F_{\rm sph}(Qr)\,{\rm d}r}{(R_{\max_i} - R_{\min_i})}, \quad (7)$$

where

$$IQ_{0i} = \frac{(\rho_1 - \rho_2)^2 \varphi}{\overline{V_r}} f(r_i)(R_{\max_i} - R_{\min_i}) \quad (8)$$

is the contribution to $I(Q)$ of the ith histogram cell which has limits $R_{\min_i}$ and $R_{\max_i}$.

The program fits equation (7) to the $I(Q)$ curve using *Excel*'s Solver addin. As with the fractal distribution fit, a separate *Excel* worksheet is created and the fit is carried out with Solver. A number of macros programmed into the worksheet aid the fitting procedure, which can be a bit tricky, and calculate properties once a satisfactory fit is obtained. These properties include the porosity and the specific surface area (assuming a porous sample). The porosity can be calculated from equation (8).

The specific surface area for probe size r is calculated from the pore size distribution as the sum of surface areas of all pores, of radius larger than r, divided by the sample volume,

$$\frac{S(r)}{V} = n_v \int_r^{R_{\max}} A_r f(r')\,{\rm d}r', \quad (9)$$

where n_v is the average number of pores per unit volume,

$$n_v = \frac{\varphi}{\overline{V_r}} = \frac{I(0)}{(\rho_1 - \rho_2)^2} \frac{1}{\overline{V_r^2}}.$$

$S(r)$ is the total surface area of pores with radius larger than r, and $A_r = 4\pi r^2$.

The procedure has been tested with synthetic fractal data to ensure that it works correctly. It is used routinely in our work on porous media (Radlinski, Kennard *et al.*, 2004; Radlinksi, Mastalerz *et al.*, 2004; Ioannidis *et al.*, 2004; Radlinski, Ioannidis *et al.*, 2004). As a further test, a bimodal distribution for the volume-weighted $f(r)$ distribution $[r^3 f(r)]$ was simulated and an $I(Q)$ produced using equation (7). The $I(Q)$ curve was analysed using the histogram fitting procedure. The results are shown in Fig. 2.

Fig. 2(*a*) shows the generated $I(Q)$ data and the fitted $I(Q)$ curve after two iterations of the fitting procedure. Each iteration involves running Solver to find the minimum sum of squared errors (SSQ). Before each iteration, an initial guess is produced by 'flattening' the fitted $f(r)$ distribution using an *Excel* macro called 'FlattenIQ0'.

Fig. 2(*b*) shows $f(r)$ after one and two iterations on a log–log scale. The specific surface area and sensitivities, expressed as $\Delta({\rm SSQ})/\Delta\log(IQ_{0i})$, are also plotted, as normally provided by the program. The simulated $f(r)$ is plotted for comparison.

Despite the apparently poor comparison between the simulated $f(r)$ and fitted $f(r)$, the procedure produces a very good result when the original volume-weighted $f(r)$ is compared with that produced by the program. Fig. 2(*c*) shows these two curves, along with the points produced after one iteration, on a linear scale. The fitted $r^3 f(r)$ curve for two iterations was scaled up by a factor of 2.5 to match the simulated curve and compensate for the different normalizing factors in the $f(r)$.

This example also serves to show that some care must be taken to find the fit that is most likely to correspond to the global minimum. If Solver is run only once, the $f(r)$ curve has a noticeable gap near $\log(r) = 2.6$ (Fig. 2*b*) and the corresponding $r^3 f(r)$ curve is very erratic (Fig. 2*c*). The second iteration produces a relatively smooth $f(r)$ curve. Further iterations do not improve the fit. In the author's experience, running Solver more than once, without flattening the

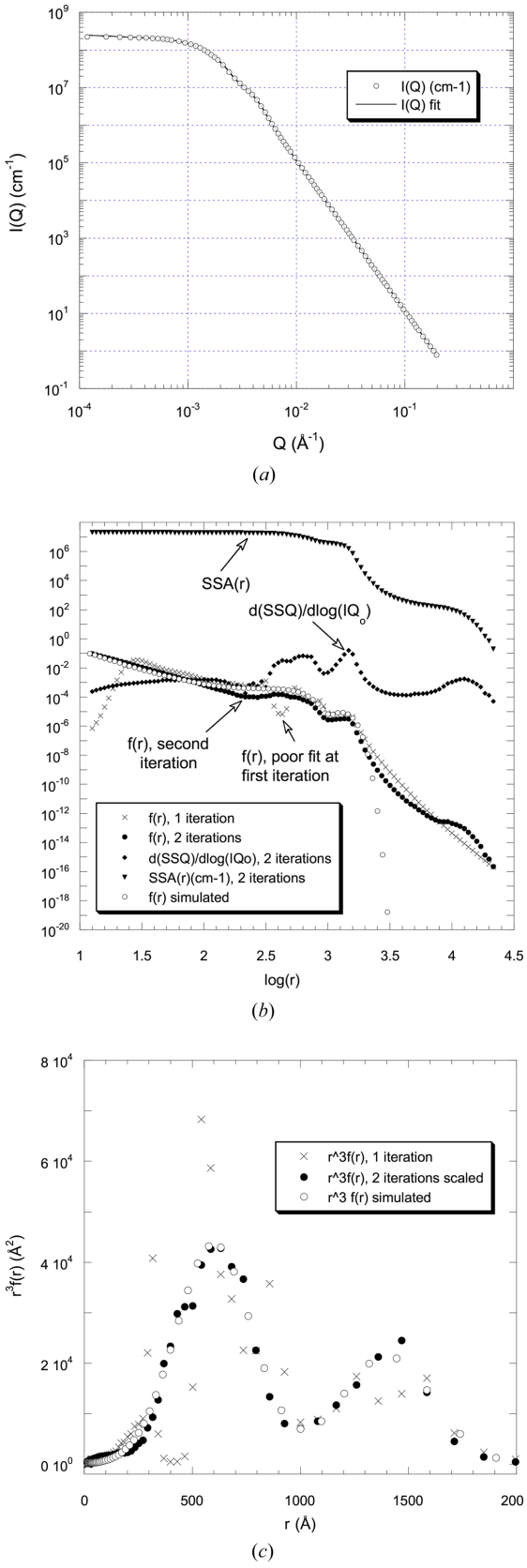

Figure 2
Histogram fit applied to a simulated bimodal distribution for $r^3 f(r)$. (*a*) $I(Q)$ curve calculated from the simulated distribution and $I(Q)$ obtained by fitting a histogram; (*b*) $f(r)$, SSA(r) and $\Delta({\rm SSQ})/\Delta\log(IQ_0)$ obtained after two iterations, compared with $f(r)$ after one iteration and the simulated $f(r)$; (*c*) $r^3 f(r)$ obtained after two iterations compared with one iteration and the simulated distribution.

initial guess, leads to less-smooth $f(r)$ curves and it is suggested that the optimum fit is obtained when the $f(r)$ curve, on a log–log scale, appears smooth. Solver, itself, does not provide any indication of whether a global minimum has been found, nor any indication of the errors in the fit.

3.3.7. Correlation function. The correlation function is related to $I(Q)$ by the following equation,

$$\gamma(r) = \frac{1}{C_0 2\pi^2} \int_0^\infty Q^2 I(Q) \frac{\sin(Qr)}{Qr}\, \mathrm{d}Q. \qquad (10)$$

A plot of the correlation function can be displayed in a separate window. In the window, the values of C_0 and density contrast can be entered and the program will calculate a corresponding value of porosity using the value of r_0 (the correlation at $r = 0$). C_0 is unity for neutrons and I_e^2 for electrons ($I_e = e^2/mc^2 = 2.82 \times 10^{-13}$ cm is the scattering amplitude of a single electron).

3.3.8. Vitrinite reflectance *versus* $I(Q)$. If vitrinite reflectance values have been entered into the SASProc database (for example, for organic-rich sedimentary rocks), plots of vitrinite reflectance *versus* $I(Q)$, for a specific value of Q, and a selected set of rock samples, can be produced.

3.3.9. Depth *versus* $I(Q)$. If depth values have been entered into the SASProc database (for example, for rock samples obtained from well cores), plots of depth *versus* $I(Q)$, for a specific value of Q, and a selected set of rock samples, can be plotted.

3.3.10. Printing and output. In addition to some basic printing ability, the program allows the exporting of data and plots to *Excel* workbooks for further analysis.

3.3.11. Synthetic mercury injection curve. An emulated mercury injection curve can be obtained. Values of pressure of mercury and corresponding values for percent volume of pore space occupied by the mercury are calculated.

4. Hardware requirements

The program was designed to run on a Windows-based personal computer. Windows 95 or Windows NT or later, with 64 Mbyte of RAM, or better, is recommended. Although the program runs satisfactorily on a Pentium 200, a faster processor is recommended as the embedded Microsoft *Excel* charts require much background processing.

5. Conclusion

Small-angle neutron scattering and small-angle X-ray scattering are becoming increasingly important tools for studying the structure of rocks and other materials. It is therefore of benefit to minimize the time required to process and interpret the raw scattering data. This is achieved by the program *PRINSAS* by taking advantage of the interactive environment of a Windows-based personal computer and the database capabilities of Microsoft *Access*.

Thanks are given to Andrzej Radlinski for assistance in preparing this text, to Elliot Gilbert and Chris Garvey at ANSTO for trying out *PRINSAS*, to Peter Petkovic and Frank Brassil for helpful suggestions, and to the referees for their helpful criticism and comments.

References

Bale, H. D. & Schmidt, P. W. (1984). *Phys. Rev. Lett.* **53**, 596–599.
Espinat, D. (1990). *Application des Techniques de diffusion de la Lumiere, des Rayons X et des Neutrons a l'Etude des Systemes Colloidaux.* Revue de l'Institut Francais du Petrole, Vol. 45, No. 6, pp. 1–131.
Guinier, A., Fournet, G., Walker, C. B. & Yudowitch, K. L. (1955). *Small-Angle Scattering of X-rays*. New York: John Wiley.
Hinde, A. (2002). *PRINSAS – a Windows-based program for processing and interpreting small-angle neutron and X-ray scattering data*, http://www.ga.gov.au/about/corporate/ga_authors/publications_free.jsp#Marine.
Ioannidis, M. A., Amirtharaj, E. S., Macdonald, I. F., Radlinski, A. P., Hinde, A. L. & Tsakiroglou, C. D. (2004). *Chem. Eng. Sci.* Submitted.
Lake, J. A. (1967). *Acta Cryst.* **23**, 191–194.
Lindner, P. & Zemb, T. (1991). Editors. *Neutron, X-ray and Light Scattering.* Amsterdam: Elsevier.
Mildner, D. F. R. & Hall, P. L. (1986). *J. Phys. D*, **19**, 1535–1545.
Radlinski, A. P., Boreham, C. J., Wignall, G. D. & Lin, J.-S. (1996). *Phys. Rev. B*, **53**, 14152–14160.
Radlinski, A. P. & Hinde, A. L. (2001). *Proceedings of the ESRF/ILL Workshop on Environmental Studies Using Neutron and Synchrotron Facilities*, 20–21 February 2001, chaired by Å. Kvick, p. 11. European Synchrotron Radiation Facility, Grenoble, France.
Radlinski, A. P., Ioannidis, M. A., Hinde, A. L., Hainbuchner, M., Baron, M., Rauch, H. & Kline, S. R. (2004). *J. Colloid Interface Sci.* **274**, 607–612.
Radlinski, A. P., Kennard, J. M., Edwards, D. S., Hinde, A. L. & Davenport, R. (2004). *APPEA J.* pp. 151–180.
Radlinksi, A. P., Mastalerz, M., Hinde, A. L., Hainbuchner, M., Rauch, H., Baron, M., Lin, J. S., Fan, L. & Thiyagarajan, P. (2004). *Coal.* **59**, 245–271.
Radlinski, A. P. & Radlinska, E. Z. (1999). *Coalbed Methane: Scientific, Environmental and Economic Evaluation*, edited by M. Mastalerz, M. Glikson & S. D. Golding, pp. 329–365. Dodrecht: Kluwer.
Sabine, T. M. & Bertram, W. K. (1999). *Acta Cryst.* A**55**, 500–507.
Schelten, J. & Schmatz, W. (1980). *J. Appl. Cryst.* **13**, 385–390.
Schmidt, P. W. (1989). *The Fractal Approach to Heterogeneous Chemistry*, edited by D. Avnir, pp. 67–79. New York: John Wiley.
Strunz, P., Saroun, J., Keiderling, U., Wiedenmann, A. & Przenioslo, R. (2000). *J. Appl. Cryst.* **33**, 829–833.
USANS User Manual (1999). Version 1.0, January 1999, 01/06/98. Oak Ridge National Laboratory, Tennessee, USA.
Wong, P.-Z., Howard, J. & Lin, J.-S. (1986). *Phys. Rev. Lett.* **57**, 637–640.